Journal of Korean Society of
Coastal and Ocean Engineers
Vol. 20, No. 1, pp. 93~100, February 2008

Calculations of Storm Surges, Typhoon Maemi
해일고 산정 수치모의 실험, 태풍 매미

Jong-Chan Lee*, Jae-Il Kwon*, Kwang-Soon Park*, and Ki-Cheon Jun*
이종찬* · 권재일* · 박광순* · 전기천*

Abstract : A multi-nesting grid storm surge model, Korea Ocean Research and Development Institute-Storm surge model, was calibrated to simulate storm surges. To check the performance of this storm surge model, a series of numerical experiments were explored including tidal calibration, the influence of the open boundary condition, the grid resolutions, and typhoon paths on the surge heights using the typhoon Maemi, which caused a severe coastal disasters in Sep. 2003. In this study the meteorological input data such as atmospheric pressure and wind fields were calculated using CE wind model. Total 11 tidal gauge station records with 1-minute interval data were compared with the model results and the storm surge heights were successfully simulated. The numerical experiments emphasized the importance of meteorological input and fine-mesh grid systems on the precise storm surge prediction. This storm surge model could be used as an operational storm surge prediction system after more intensive verification.

Keywords : storm surge model (kordi-s), CE wind model, typhoon Maemi

요 지 : Multi-nesting grid system을 이용한 한국해양연구원의 해일모델을 해일고 산출에 사용하기 위해 검증하였다. 다양한 수치실험은 2003년 9월 내습한 태풍 매미를 기준으로 이루어졌다. 이 태풍해일모델의 성능을 알아보기 위해 조석검증을 비롯하여 개방경계조건, 격자 크기 그리고 태풍의 진로 등에 대한 일련의 수치실험이 실시되었다. 본 연구에서 기상입력자료인 해면기압장과 바람장은 CE wind 모델로 계산하였다. 총 11개 조위관측소의 1분 간격 조위자료와 모델 결과를 비교하였으며, 해일고를 성공적으로 재현하였다. 이러한 실험들은 정밀한 해일고 산출에 있어 기상자료의 중요성과 상세정밀격자의 필요성을 강조하기 위한 것이다. 이 태풍해일 모델은 보다 세밀한 검증과정을 거친다면 해일고 예측을 위해 상시 운용될 수 있다고 사료된다.

핵심용어 : 폭풍해일모델(한국해양연구원 해일모델), CE wind 모델, 태풍 매미

1. Introduction

Storm surges are oscillations of the water level in a coastal or inland water body forced by the atmospheric weather system (Murty, 1984). Abnormal high waters have been caused tremendous damages in the coastal regions around the world such as North Sea flood (1953) in Europe, typhoon Isewan (1959) in Japan, typhoon Maemi (2003) in Korea, hurricane Katrina (2005) in USA. Moreover, the recent studies have warned that global warming related to the climate change will rise the sea level and will cause more powerful tropical cyclones. To mitigate and to prevent coastal disasters induced by storm surge, an accurate and fast storm surge prediction system is required. In this paper we developed Korea Ocean Research and Development Institute-Storm surge model (KORDI-S) and introduced its basic structures and performances for storm surge prediction.

For various numerical experiments, typhoon Maemi was chosen because of two reasons. First, typhoon Maemi was almost the first typhoon that was recorded with 1-minute interval at the tidal gauge stations operated by National

*한국해양연구원 연안개발연구본부(Corresponding author: Jae-Il Kwon, Coastal Engineering Research Department, Korea Ocean Research and Development Institute, Ansan P.O. Box 29, Seoul 426-600, Korea, jikwon@kordi.re.kr)

Oceanographic Research Institute (NORI) in Korea. In previous most of storm surge records were based on the 1-hour interval data which are easy to miss the real peak because of fast passing of the typhoons. Second, typhoon Maemi recorded not only tremendous economic loss but also historic weather survey in Korea. In Masan city, residential and commercial areas, which are far from the Masan Port, were flooded by the severe storm surge (about 2.1 m). Several numerical simulations for storm surge by typhoon Maemi were conducted (Choi et al., 2004; Kang, 2004; Kawai et al., 2005; Moon et al., 2007).

In this study, first we calibrated KORDI-S for tides and then checked its performance to predict storm surges by given various conditions such as 1) different open boundary conditions, 2) horizontal resolution effects by using nesting grid system, 3) importance of the typhoon track. All model results (east and south coasts) were compared with the observed storm surge data (total 11 tidal gauge stations, see Fig. 1). In Chapter 2 the numerical experiments were described and model results were discussed in Chapter 3. Summary and conclusions were given in Chapter 4.

2. Numerical Experiments

2.1 Numerical model

Numerical experiments were carried out to simulate typhoon Maemi using a numerical storm surge model (KORDI-S). The applied KORDI-S (2D version) was based on continuity equation and depth-averaged momentum equations (Eqs. 1-3).

$$\frac{\partial \zeta}{\partial t}+\frac{\partial (Hu)}{\partial x}+\frac{\partial (Hv)}{\partial y}=0 \tag{1}$$

$$\frac{\partial u}{\partial t}-fv=-\frac{1}{\rho}\frac{\partial P_a}{\partial x}-g\frac{\partial \zeta}{\partial x}+\frac{\tau_x^w-\tau_x^b}{\rho H}+F_x \tag{2}$$

$$\frac{\partial v}{\partial t}+fu=-\frac{1}{\rho}\frac{\partial P_a}{\partial y}-g\frac{\partial \zeta}{\partial y}+\frac{\tau_y^w-\tau_y^b}{\rho H}+F_y \tag{3}$$

where ζ is the sea surface elevation, H is the total water depth ($=h+\zeta$), h is the still water depth below the mean sea level, t is time, g is the gravitational acceleration, ρ is the sea water density, P_a is the atmospheric pressure at the mean sea level, f is the Coriolis parameter, $\vec{\tau}^w$ is the wind stress, $\vec{\tau}^b$ is the bottom stress, $\vec{F}$ is the sum of advection and diffusion term, u and v the flow velocities in x and y directions, respectively.

A staggered grid (Arakawa C grid) system, which gave spatial second order accuracy, was used. A fully implicit scheme was implemented with a conjugate gradient method (Strikwerda, 1989) for a large sparse matrix solver. Horizontal advection terms were treated explicitly using sum of two other second-order difference schemes (Stelling, 1984). An one-way multi-nesting scheme was used to resolve complex coastal topograph and uncertain open boundary conditions. The initial values for surface elevation and flow velocities at the entire domain were all set to zero and at the land boundaries no-slip condition was applied.

The wind stress, $\vec{\tau}^w$ and the bottom stress, $\vec{\tau}^b$ are set to be the quadratic relationships (Eqs. 4 and 5, respectively) and the Wu (1980)'s wind drag coefficient is used.

$$(\tau_x^w, \tau_y^w)=\rho_{air} C_d \sqrt{W_x^2+W_y^2}(W_x, W_y) \tag{4}$$

$$(\tau_x^b, \tau_y^b)=\rho C_f \sqrt{u^2+v^2}(u, v) \tag{5}$$

where $\vec{W}$ is wind speed, C_d is the wind drag coefficient ($=(0.8+0.065|W|)*10^{-3}$), ρ_{air} is the air density. In this study we use two values of the bottom drag coefficients, C_f. Where higher than 33°N and shallower than 100 m, 0.001 was used and rest of area was set to 0.0025.

The horizontal wind velocities at a height of 10 m above the sea surface were calculated by CE (U.S. Army Corps of Engineers) wind model which will be described later.

2.2 Multi-nesting grid system

In the model, 3-step nesting grids were used (Fig. 1). The first domain (D10) covered the entire Yellow Sea and the East China Sea with 1/12°×1/12° grid resolution. The second domain (D20) covered 33-39°N, 125-130°E with 1/60°×1/60° grid resolution. The D10 and D20 domains were solved under a spherical coordinate system. The third domain (D30), where 3 tidal stations (Tongyoung, Masan and Busan) were included, was discretized with a 300 m× 300 m finer grid under a Cartesian coordinate system.

The sea surface elevations along open boundaries in the D10 were specified using an inverse barometric pressure. In this study, tidal influences on storm surge were not considered, however, tidal calibration was carried out to check the model's performance. Major four tidal constituents, M_2, S_2, K_1 and O_1, were given at the open boundaries simulta-

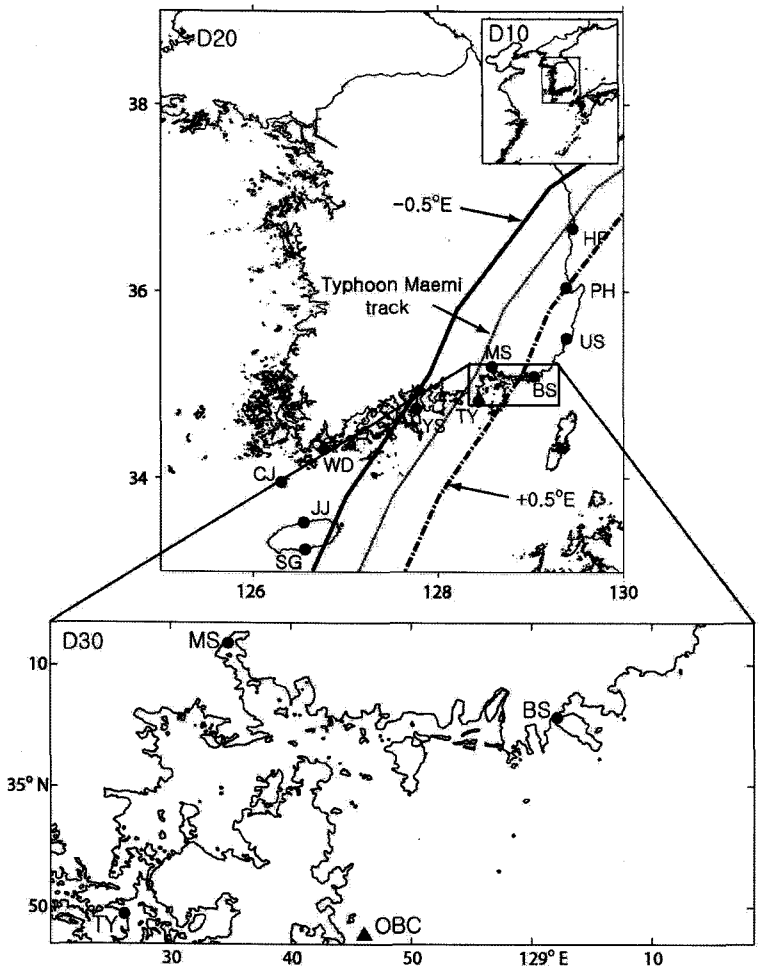

Fig. 1. Model domains (D10, D20, and D30). In the middle panel the original track, east shifted track, and west shifted track of typhoon Maemi were represented. 11 tidal gauge stations were marked with closed circles.

neously and ran more than 15 days. The observed tidal constituents were calculated using 1-year length sea surface elevation data with 1-hour interval records from NORI (total 26 tidal station around the Korea coasts). The comparisons of model calculated and observed tidal constituents (M_2 and S_2) were quite close and there was not much difference between D10 and D20 (Fig. 2). In terms of M_2, the finer grid (D20) showed generally better agreements but in Mokpo D10 (145.0 cm) was more close than D20 (166.6 cm) to the observed value (141.9 cm). Meantime, relatively big differences of S_2 phase were shown in Hupo and Pohang because those sites located close to the amphidromic point of S_2 (less than 5 cm of amplitude).

It should be noted that K_1 and O_1 were shown similar results (not presented in the Figures). Numerical experiments with and without tidal elevations, derived using M_2, S_2, K_1 and O_1 constituents, gave almost same surge heights in the D30, where a tidal range was relatively small compared with that of the west coast of Korea. The approximate highest high water (M_2+S_2+K_1+O_1) in Masan is less than 100 cm. The open boundary sea surface elevations in the D20 (D30) were specified by interpolating the D10 (D20) modeled sea surface elevations spatially and temporarily.

2.3 CE wind model for the meterological input data

The meteorological inputs (atmospheric pressure and wind fields) for storm surge were calculated by a paramet-

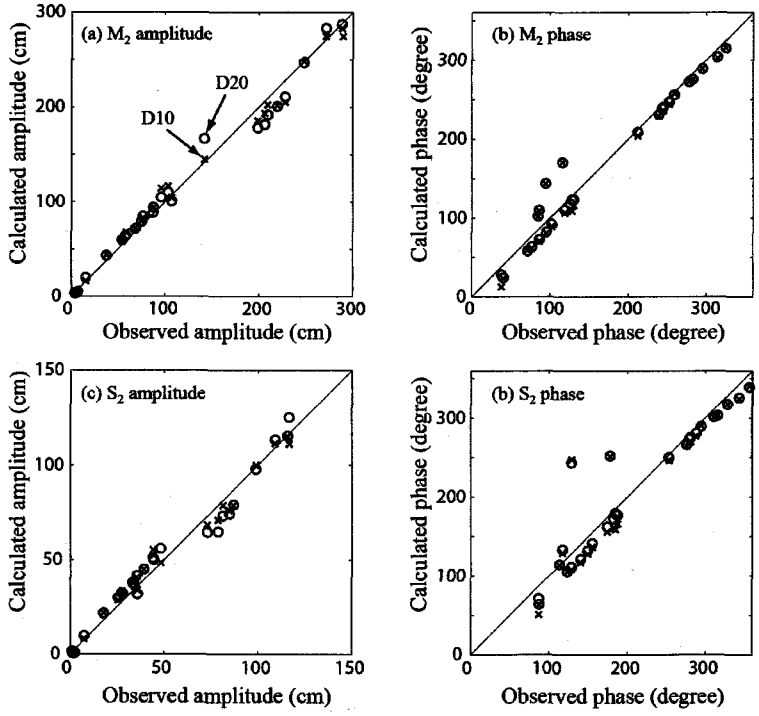

Fig. 2. *The comparisons of model calculated and observed two tidal constituents along the Korean coasts. D10 and D20 were marked with crosses and circles, respectively.*

Table 1. Typhoon Maemi track information (KMA, 2003)

Date (GMT)	Location of typhoon center		Central Pressure (hPa)	R_{max} (km)
	Latitude (N)	Longitude (E)		
8-Sep-2003 06:00	20.1	132.9	975	60
9-Sep-2003 06:00	22.4	129.4	950	60
10-Sep-2003 00:00	23.7	127.4	925	60
10-Sep-2003 12:00	24.3	126.0	915	60
11-Sep-2003 01:00	25.3	125.1	910	60
11-Sep-2003 06:00	25.8	125.2	915	60
11-Sep-2003 12:00	26.8	125.4	930	60
11-Sep-2003 18:00	28.5	125.8	935	60
11-Sep-2003 21:00	29.5	126.1	940	60
12-Sep-2003 00:00	30.5	126.5	945	60
12-Sep-2003 03:00	31.6	126.7	945	60
12-Sep-2003 06:00	32.7	127.0	950	75
12-Sep-2003 09:00	33.8	127.5	950	75
12-Sep-2003 12:00	35.1	128.4	955	85
12-Sep-2003 15:00	35.8	128.7	960	85
12-Sep-2003 18:00	37.1	129.7	970	85
12-Sep-2003 21:00	37.8	130.7	970	85
13-Sep-2003 00:00	38.6	131.7	975	110
13-Sep-2003 06:00	40.5	134.5	980	150
13-Sep-2003 12:00	42.3	138.1	980	150

ric typhoon model, namely CE (U.S. Army Corps of Engineers) wind model. The major inputs for CE wind model were locations of typhoon center, central atmospheric pressure and R_{max} (radius for maximum wind speed). Detailed descriptions of CE wind model could be found in Cardone et al. (1992), Thompson and Cardone (1996), and Kang et al. (2002). The hourly-interpolated meteorological inputs were based on KMA's typhoon information (Table 1) and used in the storm surge model for each grid system. Wind drag coefficients were calculated with Wu (1980)'s formula.

3. Model Results

Numerical experiments can be summarized as follows: 1) influences of open boundary on storm surge heights with the track of typhoon Maemi. 2) sensitivities of the typhoon Maemi's path, and 3) the grid resolution. All results were compared with observed storm surge heights. Storm surge heights were defined by observed sea level minus predicted tidal level, where tidal elevations were predicted using 64 harmonic constituents based on 1 year record.

3.1 Influence of open boundary condition

It is very important to treat open boundary conditions correctly, when a meteorological forcing is involved, if a storm surge warning system will be operated. To check the influence of open boundary condition we specified the sea surface elevations along open boundaries 1) using the nesting grid system and 2) using an inverse barometric pressure (IBP) directly at the D30 boundaries. The open boundary condition on the nesting grid system was set only in D10 with an inverse barometric pressure relationship and D20 (D30) were used the results of D10 (D20) at the boundaries. Fig. 3 showed that surge heights located about 1 km away from the boundaries (see triangle mark in the lower panel of Fig. 1). The storm surge, calculated by IBP method directly (see the thick dash-dot line in Fig. 3), was smaller than that of using the nesting grid (see the thick solid line in Fig. 3). However, it was quite similar to the simple calculation of inverse barometric pressure that described in Eq. 6 (see the thin dotted line in Fig. 3).

$$\zeta = \frac{(\bar{P} - P_a)}{\rho g} \tag{6}$$

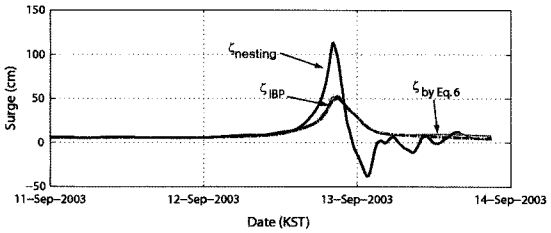

Fig. 3. Calculated sea surface elevations at the near open boundary in D30 (see the triangle mark in the lower panel of Fig. 1). Thick solid, thick dash-dot, and thin dotted lines represented multi-nesting grid, open boundary condition using IBP, and calculation using Eq. 6, respectively.

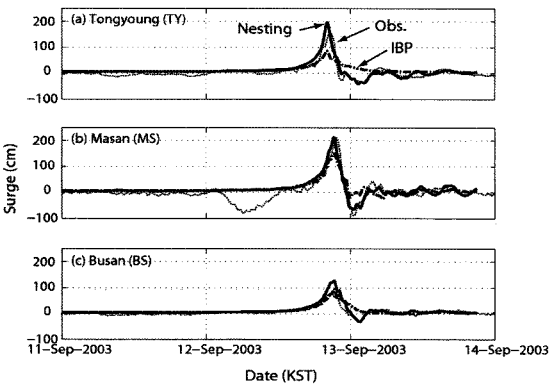

Fig. 4. Comparison of open boundary schemes. The storm surge heights of observed (thin dotted lines), by multi-nesting grid (thick solid lines), and IBP (thick dash-dot lines) are represented.

where $\bar{P}$ is the reference atmospheric pressure, 1015 hpa.

The influences of open boundary elevation on the maximum surge heights in Tongyoung, which locates near open boundary, were clearly; The surge heights calculated without nesting grid were underestimated, those with nesting grid were overestimated (Fig. 4). In Masan, the maximum surge heights calculated without nesting grid were underestimated 50 cm approximately, those with nesting grid were almost same to observation. However, the maximum surge heights in Busan were overestimated when nesting grid was used. For an operational storm surge warning system, it might be necessary to use a nesting grid to reduce uncertainties in open boundary condition.

3.2 Sensitivities of typhoon path

To check the sensitivities of typhoon path on the storm surge heights the typhoon Maemi track (see dotted line in

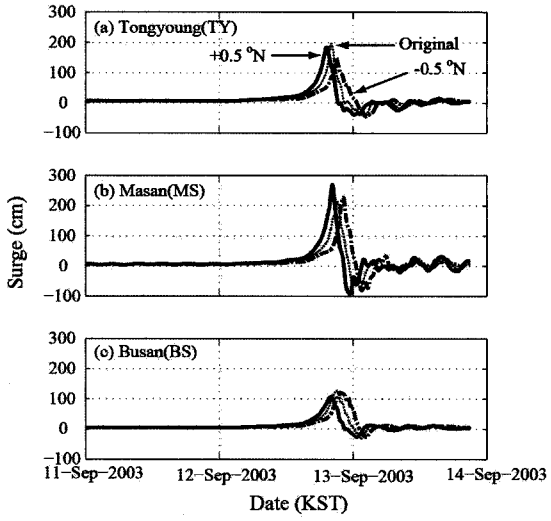

Fig. 5. Effect of shifting typhoon track in north-south direction with the original track's surge heights. The time series of storm surge heights by the original track (thin dotted lines), northward shift (thick solid lines), and southward shift (thick dash-dotted lines) tracks were represented.

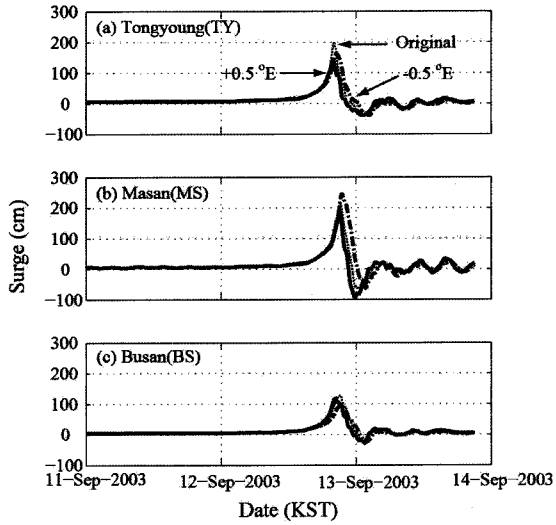

Fig. 6. Effect of shifting typhoon track in East-West direction with the original track's surge heights. The time series of storm surge heights by the original track (thin dotted lines), eastward shift (thick solid lines), and westward shift (thick dash-dot lines) tracks were represented.

the middle panel of Fig. 1 and Table 1) was shifted to 0.5 degree toward North, South, East and West, respectively. All meteorological inputs were re-calculated by using CE wind model for the domain of D10, D20 and D30. The calculated storm surges in D30 with shifting tracks in north-south direction were shown in Fig. 5; When track was shifted to the north (south), the maximum surge height occurred early (late) compared with the observations.

In Fig. 6 the calculated storm surges with shifting tracks in east-west direction were represented; When the track was shifted to the east (thick dash-dot line in the middle panel of Fig. 1), the maximum surge heights in Tongyoung, Masan, Busan were underestimated than those from the original track. When the path was moved to the west (thick solid line in the middle panel of Fig. 1), only Masan showed the higher maximum storm surge height and those in Tongyoung and Busan dropped down. The maximum storm surge heights in Masan reached about 245 (185) cm when the typhoon path was shifted to the east (west). The experiments clearly showed that how the typhoon path is critical to the storm surge prediction. When the typhoon passed to the left (right) side of tidal stations, the maximum storm surge heights became higher (lower). However, how much the change could not be simply determined by the distance between the typhoon path and tidal stations because of the combined effect of the radius for maximum wind speed (R_{max}) and the complex geometry.

Because Yeosu and Wando were not included in D30, we analyzed the model responses using results in D20. It turned out that Yeosu was the most sensitive on track shifting (east-west) giving the maximum storm surge heights differences about 90 cm. Meantime, Wando was about 68 cm.

It should be noted that the highest storm surge heights occurred in Masan within 1° range shifting of the original track of typhoon Maemi in east-west and north-south directions. For the occurrence time differences of the maximum storm surge heights were about 40 minutes (east-west) and about 2 hours (north-south).

3.3 Sensitivities of grid resolution

There were other observation sites. Here we compared model results in D10 and D20 with other places. Except Yeosu the surge heights of other sites were less than 100 cm, Yeosu (Fig. 7d) was plotted with different y-axis scale. Fig. 7(a-c) showed storm surge in the east coast of Korea (see Fig. 1 for location of all tidal stations), where a weak tide occurs, with observations. The surge heights in Pohang, which can not be resolved properly by 1/12°×1/12° grid

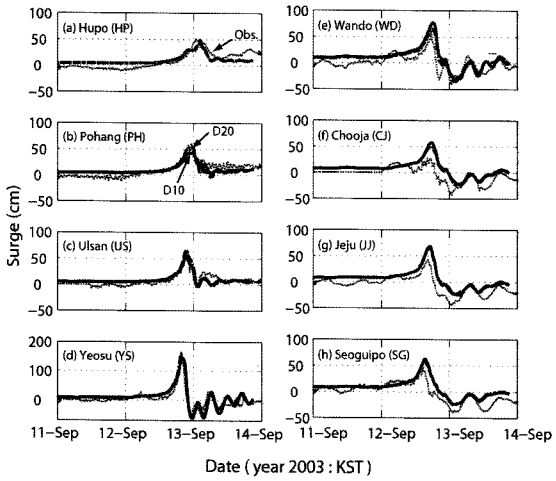

Fig. 7. Influences of grid resolutions on surge heights with the original track of typhoon Maemi. Observed (solid line) and calculated storm surges using D10 (dash line) and D20 (dash-dot line) are represented.

resolution, were slightly different according to grid resolutions. Maximum surge heights in D20 were slightly larger than those in D10. Calculations of KORDI-S showed a quite good agreement to the observations. Fig. 7(d-f) showed storm surge in the southwest coast of Korea with observations (The tidal stations located left side of the typhoon center). In these regions, maximum surge heights in D20 were slightly smaller than those in D10, and the surge heights were overestimated.

It should be noticed that the finer grid with nesting scheme gave the better results of the typhoon Maemi. For instance, the maximum surge heights in Masan are 211 cm (observed), 194 cm (D10), 200 cm (D20), 213 cm (D30), respectively.

4. Summary and Conclusions

In this study we carried out a series of numerical experiments to calibrate and verify the KORDI-S for storm surge simulation using the typhoon Maemi (Sep. 2003). To overcome the difficulties in open boundary condition, an one-way multi-nesting scheme was used in a storm surge model, giving reasonable results. Model results were sensitive to meteorological forcing, which were calculated from CE wind model.

A series of numerical experiments showed that 1) the performances of the KORDI-S in terms of the hydrodynamic including storm surges were reasonable, 2) the most important factor in the calculations of storm surge was the location of typhoon center (i.e. track), 3) storm surge heights could be simulated correctly if a reliable typhoon track is available, and 4) the finer grid simulated storm surge heights correctly in the area of the relatively complex geometry, and 5) using nesting grid could reduce uncertainties in the open boundary condition. Therefore, if the meteorological input is precise enough, the KORDI-S can be used as an operational storm surge prediction system after more hindcasting of historic events.

Acknowledgements

This study was conducted in the fulfillment of "Top Brand Project: Development of operational fine-mesh storm surge prediction system (PE98060)" from Korea Ocean Research and Development Institute.

References

Cardone, V.J., Cox, A.T. Greenwood, J.A. and Thompson, E.F. (1992). Upgrade of Tropical Cyclone Surface Wind Field Model, CERC-94-14, U.S. Army Corps of Engineers.

Choi, B.H., Eum, H.M., Kim, H.S., Jeong, W.M. and Shim, J.S. (2004). Wave-Tide-Surge Coupled Simulation for Typhoon Maemi, Waves and Storm Surges around Korean Peninsula, Special Workshop on Korean Society of Coastal and Ocean Engineers, 121-144.

Kang, S.W., Jun, K.C., Park, K.S. and Bang, G.H. (2002). A Comparison of Typhoon Wind Models with Observed Winds, The Sea, J. of the Korean Soc. Of Oceanogr. 7(3), 100-107 (in Korean).

Kang, Y.Q. (2004). Storm Surge Resonance During the Passage of Typhoon 'Maemi', Special Workshop on Korean Society of Coastal and Ocean Engineers, 57-62 (in Korean).

Kawai, H., Kim, D.-S., Kang, Y.-K., Tomita, T. and Hiraishi, T. (2005). Hindcasting of Storm Surge at Southeast Coast by Tphoon Maemi, The Korean Society of Ocean Engnieering, 19(2), 12-18.

Korea Meteorological Administration (2003). Typhoon Maemi White Paper (in Korean).

Moon, S.-R., Kang, T.-S., Nam, S.-Y. and Hwang, J. (2007). A study on Scenario to establish Coastal Inundation Prediction Map due to Storm Surge, Korean Society of Coastal

and Ocean Engineers, 19(5), 492-501 (in Korean).

Murty, T.S. (1984). Storm Surges-meteorological ocean tides, Canadian Bulletin of Fisheries and Aquatic Sciences, Ottawa.

Stelling, G.S. (1984). On the construction of computational methods for shallow water flow problems. Rijkswaterstaat communications, No. 35, The Hague, Rijkswaterstaat, 1984.

Strikwerda, J.C. (1989). Finite Difference Schemes and Partial Difference Equations, Wadsworth, Inc. Belmount, Calif.

Thompson, E.F. and Cardone V.J. (1996). Practical modeling of hurricane surface wind field, J. of Waterway, Port, Coastal and Ocean Engineering. 122(4), 195-205.

Wu. J. (1980). Wind-stress Coefficients Over Sea Surface Near Neutral Conditions: A Revisit, J. Phys. Oceanogr., 10, 727-740.

Received January 16, 2008
Accepted February 12, 2008